Observational Study

Medicine

OPEN

Network pharmacology and molecular docking to explore the potential molecular mechanism of chlorogenic acid treatment of oral squamous cell carcinoma

Zhanqin Feng, MSc[a], Puyu Hao, MSc[b], Yutao Yang, MSc[b], Xulong Xve, MSc[c], Jun Zhang, MSc[a,*]

Abstract

Oral squamous cell carcinoma (OSCC) is a tumor type with a high mortality rate. Chlorogenic acid, abundant in resources and widely utilized in cancer treatments, has seen limited studies regarding its efficacy against OSCC. This paper investigates chlorogenic acid's mechanism in treating OSCC, aiming to guide the development of novel drugs. The study employed network pharmacology, molecular docking, and survival analysis methods. Network pharmacological analysis revealed chlorogenic acid targets 23 OSCC-related proteins, including *ESR1, MMP2, MMP9, SRC, MAPK8, MAPK1, CDC42, ERBB2, ATM, and BRAF.* Molecular docking simulations indicated that the primary target exhibits significant binding capacity with chlorogenic acid, with *MMP9* associated with tumor migration and angiogenesis standing out. Survival analysis demonstrated that the downregulation of most primary targets correlates with improved survival rates in OSCC patients. Enrichment analysis of therapeutic targets highlighted the pivotal role of *MAPK-ERK* and *MAPK-JNK* signaling pathways in chlorogenic acid's efficacy against OSCC. This paper predicts chlorogenic acid's potential targets and proposes its molecular mechanism in treating OSCC, offering a theoretical foundation for its application in OSCC treatment. We used traditional Chinese medicine, a disease pharmacology-related information base, and an analysis platform to predict targets. The Cytoscape 3.9.1 and STING databases were used to address common targets for drugs and diseases, establish networks of protein interaction relationships, and screen core targets. Meastro11.5 was used for molecular docking simulation. R4.2.2 was used for survival analysis and joint target enrichment analysis. Network pharmacological analysis identified chlorogenic acid acting on 23 OSCC targets. Molecular docking simulations revealed a strong binding affinity of chlorogenic acid compounds with these targets, particularly *MMP9*, essential for tumor migration and angiogenesis. Survival analysis indicated that the downregulation of most core targets was correlated with improved OSCC patient survival. Enrichment analysis of therapeutic targets highlighted the critical roles of the *MAPK-ERK* and *MAPK-JNK* signaling pathways in the effectiveness of chlorogenic acid against OSCC. This study predicted the potential targets of chlorogenic acid in OSCC treatment and hypothesized its molecular mechanism, offering a theoretical foundation for its use in OSCC therapy.

Abbreviations: ACOX1 = acyl-CoA oxidase 1, AKT = protein kinase B, ARL4C = ADP ribosylation factor like GTPase 4C, ATM = ataxia-telangiectasia mutated, BP = biological process, BRAF = B-Raf proto-oncogene, serine/threonine kinase, CC = cell component, CDC42 = cell division cycle 42, ERBB2 = human epidermal growth factor receptor 2, ESR1 = estrogen receptor 1, FAK = focal adhesion kinase pathways, GO = Gene Ontology, HO-1 = heme oxygenase 1, KEGG = Kyoto Encyclopedia of Genes and Genomes, MAPK1 = mitogen-activated protein kinase 1, MAPK8 = mitogen-activated protein kinase 8, MAPK-ERK = pathways mitogen-activated protein kinases-regulated kinase pathways, MAPK-JNK = pathways mitogen-activated protein kinases -cJun NH (2)-terminal kinase pathways, MF = molecular function, MMP2 = matrix metallopeptidase 2, MMP9 = matrix metallopeptidase 9, OMIM = Online Mendelian Inheritance in Man CC cell component ESR1 estrogen receptor, OSCC = oral squamous cell carcinoma, PAIP1 = poly(A) binding protein interacting protein 1, PPI = protein–protein interaction networks, SRC = SRC proto-oncogene, TCGA = The Cancer Genome Atlas.

Keywords: chlorogenic acid, *MAPK-ERK* signaling pathway, *MAPK-JNK* signaling pathway, network pharmacology, oral squamous cell carcinoma

ZF and PH contributed to this article equally.

Supported by the Weifang Municipal Health Commission project, "Research on the effect of predicting postpartum VTE based on Improved QLD and Caprini Evaluation Models."

The authors have no conflicts of interest to disclose.

All data generated or analyzed during this study are included in this published article [and its supplementary information files].

Supplemental Digital Content is available for this article.

[a] Department of Pharmacy, Weifang Maternal and Child Health Hospital, Weifang, Shandong, China, [b] Modern Research Center for Traditional Chinese Medicine, Shanxi University, Taiyuan, China, [c] Department of Traditional Chinese Medicine, Tianjin University of Traditional Chinese Medicine, Tianjin, China.

** Correspondence: Jun Zhang, Department of Pharmacy, Weifang Maternal and Child Health Hospital, Weifang, 261000 Shandong Province, China (e-mail: shandongqiuyu@163.com).*

How to cite this article: Feng Z, Hao P, Yang Y, Xve X, Zhang J. Network pharmacology and molecular docking to explore the potential molecular mechanism of chlorogenic acid treatment of oral squamous cell carcinoma. Medicine. 2024;103:45(e40218).

Received: 28 January 2024 / Received in final form: 16 June 2024 / Accepted: 4 October 2024

http://dx.doi.org/10.1097/MD.0000000000040218

1. Introduction

Oral squamous cell carcinoma (OSCC) constitutes 90% of head and neck squamous cell carcinoma cases, exhibiting the highest incidence and mortality rates in Asia compared to other regions. The prevalence of OSCC is strongly linked to lifestyle habits, including betel nut chewing, excessive alcohol consumption, and smoking, which are prevalent in South Asia.[1] It primarily affects the tonsils and tongue of middle-aged men.[2] The standard OSCC treatment involves primary tumor resection, optionally accompanied by lymph node dissection, alongside chemotherapy and radiotherapy.[3,4] However, the effectiveness of surgical treatments is compromised by resistance to chemotherapy agents such as cisplatin (CDDP) and 5-fluorouracil, leading to unsatisfactory outcomes and a high recurrence rate.[5] This situation exacerbates the survival prospects for advanced patients with tumor metastasis, reducing their survival rate to only 34%.[6] Additionally, the absence of clinical diagnostic evidence in early-stage patients delays treatment, resulting in low survival rates, significant disability, and deteriorated quality of life among survivors. Thus, identifying new drugs and therapeutic strategies is crucial.

Chlorogenic acid, a phenolic acid compound series, is found in various plants, notably in coffee and tea.[7] It is also a key active component in numerous Chinese medicinal herbs, like honeysuckle and Eucommia, where it is utilized for its heat-clearing and detoxifying properties. Chlorogenic acid exhibits a broad spectrum of pharmacological properties, including anti-cancer, anti-diabetes, anti-obesity, antioxidant, anti-inflammatory, anti-hypertensive, antibacterial, and immune-modulating effects, making it widely applicable in food and healthcare.[8,9] Despite its benefits, the complex extraction and purification processes, poor drug stability, debates over bioavailability versus gut microbiota interactions, and potential allergic reactions to injections necessitate further clinical research and development for medicinal applications.[10,11] Its anticancer potential may stem from inhibiting cell proliferation, reducing cell viability, preventing cell invasion, enhancing cytotoxicity, and disrupting clonogenic capacity.[12] Jiang et al[13] showed that the inhibitory effect of chlorogenic acid on human oral squamous cell carcinoma cells might be due to its oxidation-mediated cytotoxic effects. It also suppresses OSCC (KB) cell proliferation by downregulating *p53* and *p21*.[14] Current research on chlorogenic acid's efficacy in treating OSCC is scant, highlighting the need for further investigation.

This paper employs a network pharmacology approach in response to this context, utilizing bioinformatics tools and systems biology principles 9 to predict chlorogenic acid's therapeutic direction for OSCC treatment.[15] It aims to holistically investigate the compound's molecular treatment mechanisms, facilitating the rapid development of novel therapeutic options for OSCC patients through in silico experiments.

2. Materials and materials

2.1. Target gene prediction of oral squamous cell carcinoma (OSCC)

Target genes for OSCC were retrieved from the GeneCards and OMIM platforms. GeneCards, a comprehensive genetic database, amalgamates information from approximately 150 gene-centric databases. "Oral squamous cell carcinoma" served as the search keyword. The GeneCards dataset was filtered using a score > 50, with higher scores indicating greater relevance to the search term. The genes identified from GeneCards and those obtained from OMIM were designated as the final disease target genes (see Table S1, Supplemental Digital Content, http://links.lww.com/MD/N777, which explains the details of the website information).

2.2. Prediction of chlorogenic acid target gene

Initially, target genes of chlorogenic acid were sourced directly from the Therapeutic Target Database, ChEMBL Database, HERB Database, and PharmMapper Database, employing an activity threshold > 6.5 and zscore > 0.6 for target gene screening. Subsequently, the PubChem database facilitated the acquisition of the 2D structure of small drug molecules, with target genes identified via SwissTargetPrediction. Genes selected from various database sources were consolidated as target genes for chlorogenic acid, with all databases specifying "Homo sapiens" as the species criterion.

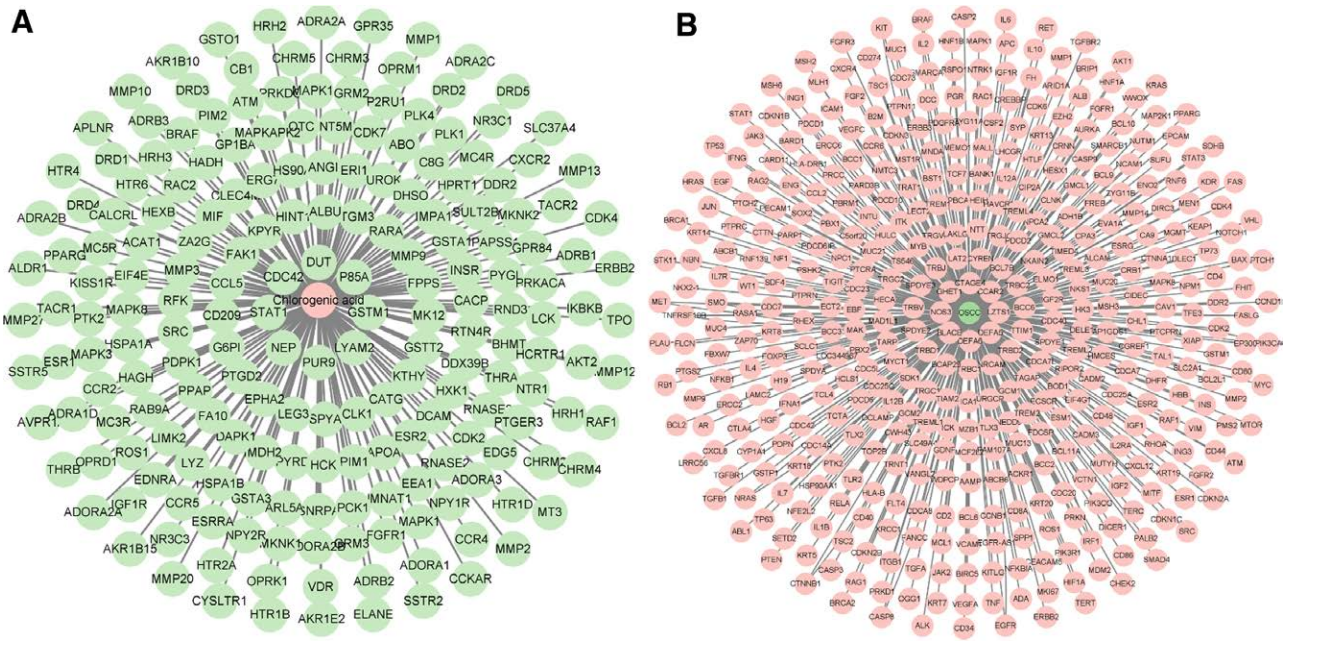

Figure 1. Maps of potential targets for drugs and diseases.

2.3. Construction and analysis of composition-target-disease network map

Critical genes for chlorogenic acid treatment of OSCC were identified by selecting common genes between drug and disease target genes. A Venn diagram, created through the Weisheng platform, visualized the expected targets, which were then utilized for further data analysis. The component-target-disease network's relationships were directly examined against drug and disease target datasets through Cytoscape visualization.

2.4. Construction of protein–protein interaction network (PPI)

The protein–protein interaction (PPI) network was derived from the STRING database, a resource built upon public

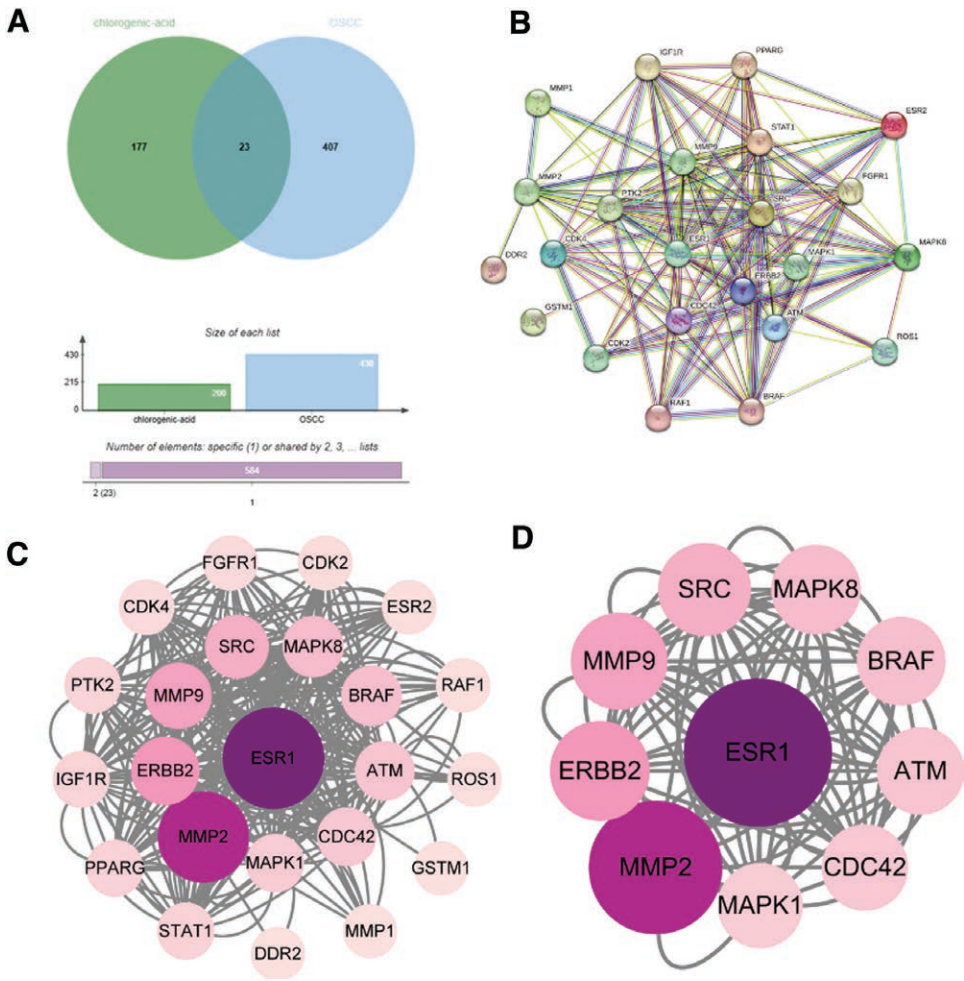

Figure 2. Core target screening and network construction. (A) Venn diagram of 200 targets of chlorogenic acid intersecting 430 targets of OSCC. (B) PPI network visualization. (C) Chlorogenic acid therapy OSCC prediction target network. The diagram has 23 nodes and 284 edges. Betweenness is used to screen for core targets. The lighter the color, the smaller the node indicates that the gene has less betweenness and less interaction with other targets; conversely, the darker the color, the larger the node, the more central the gene's role. (D) Core target network, the core target with the top 10 betweenness values in the network. OSCC = oral squamous cell carcinoma, PPI = protein–protein interaction networks.

Table 1

Core target properties.

Gene	Name	Degree	Betweenness centrality	Closeness centrality
ESR1	Estrogen receptor 1	42	67.76274	0.956522
MMP2	Matrix metallopeptidase 2	36	53.430447	0.846154
ERBB2	Human epidermal growth factor receptor 2	36	19.930996	0.846154
MMP9	Matrix metallopeptidase 9	38	16.996077	0.88
SRC	SRC proto-oncogene	36	13.362742	0.846154
MAPK8	Mitogen-activated protein kinase 8	30	9.794994	0.758621
BRAF	B-Raf proto-oncogene, serine/threonine kinase	28	8.8990345	0.733333
ATM	Ataxia-telangiectasia mutated	28	7.7367964	0.709677
CDC42	Cell division cycle 42	30	6.6502886	0.758621
MAPK1	Mitogen-activated protein kinase 1	28	5.542757	0.733333

ATM = ataxia-telangiectasia mutated, BRAF = B-Raf proto-oncogene, CDC42 = cell division cycle 42, ESR1 = estrogen receptor 1, ERBB2 = human epidermal growth factor receptor 2, MAPK1 = mitogen-activated protein kinase 1, MAPK8 = mitogen-activated protein kinase 8, MMP2 = matrix metallopeptidase 2, MMP9 = matrix metallopeptidase 9, SRC = SRC proto-oncogene.

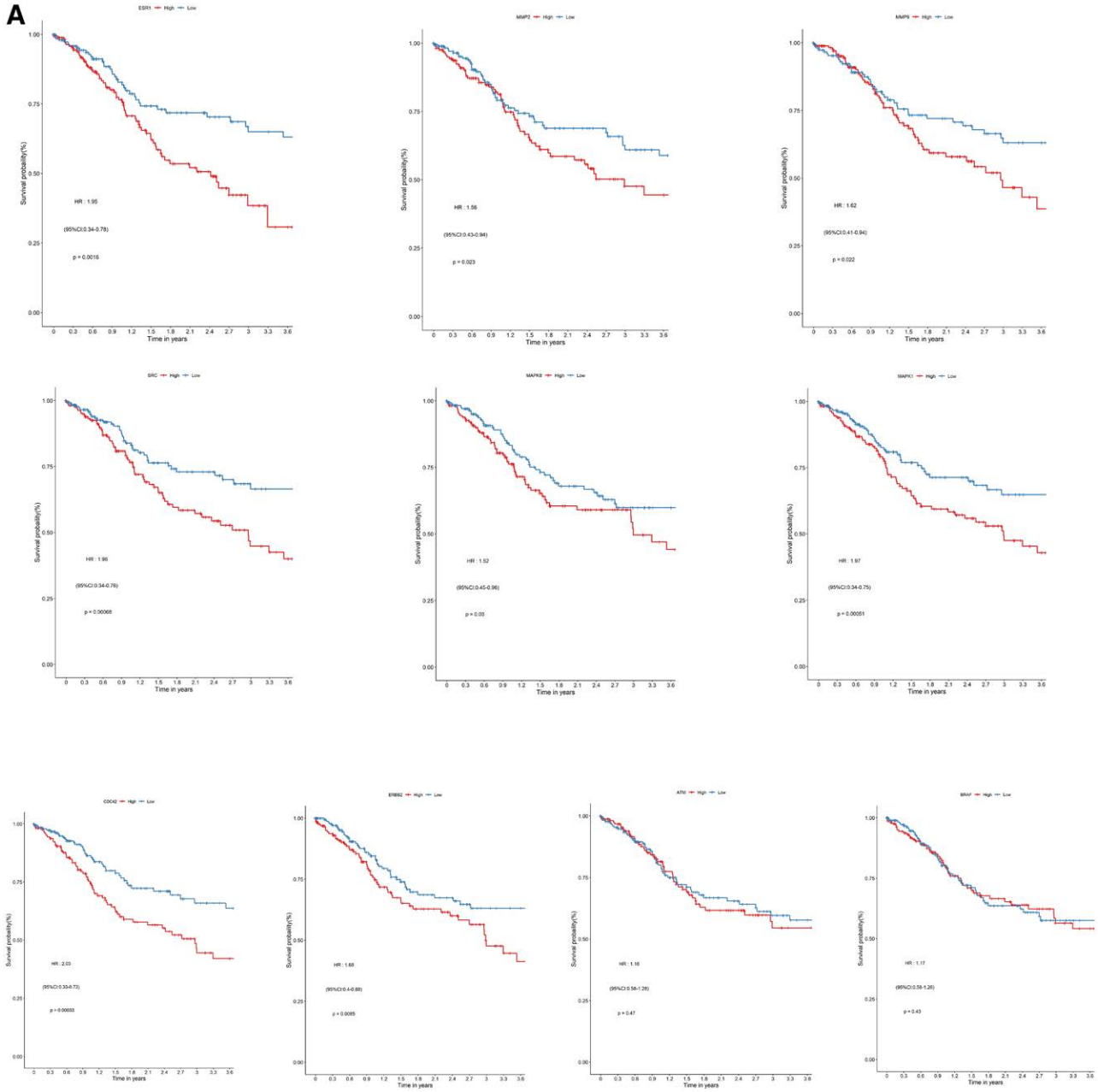

Figure 3. Gene expression was differentiated by color, with red representing the high-expression group and blue representing the low-expression group. $P < .05$ is considered as a significant difference.

databases and literature information, providing visualizations of protein interaction networks, protein families, and subcellular localization. Common targets were input as a Multiple proteins list, with "Homo sapiens" specified as the species and a medium-level confidence score (>0.400) selected to acquire protein interaction network data for the analysis of core target data.

2.5. Screening and enrichment of core targets

Protein interaction networks were analyzed with the CytoNCA plugin in Cytoscape, arranging the core targets by descending betweenness values to identify the top 10 genes. The R packages clusterProfiler, enrichplot, ggplot2, ggnewscale, DOSE, and stringr (R × 64 4.2.2) facilitated the enrichment of Gene Ontology (GO) and Kyoto Encyclopedia of Genes and Genomes (KEGG) analysis for core target genes. GO analysis was segmented into

Table 2

Molecular docking affinity score.

Gene	PDB ID	Docking score
MMP9	6esm	−10.54
ESR1	6PSJ	−7.951
ERBB2	3pp0	−7.587
ATM	7ni4	−7.426
BRAF	4mnf	−7.123
MAPK1	6g54	−6.97
MAPK8	2xrw	−6.929
CDC42	2ngr	−6.88
SRC	1is0	−5.591
MMP2	7XGJ	−4.438

ATM = ataxia-telangiectasia mutated, BRAF = B-Raf proto-oncogene, CDC42 = cell division cycle 42, ESR1 = estrogen receptor 1, ERBB2 = human epidermal growth factor receptor 2, MAPK1 = mitogen-activated protein kinase 1, MAPK8 = mitogen-activated protein kinase 8, MMP2 = matrix metallopeptidase 2, MMP9 = matrix metallopeptidase 9, SRC = SRC proto-oncogene.

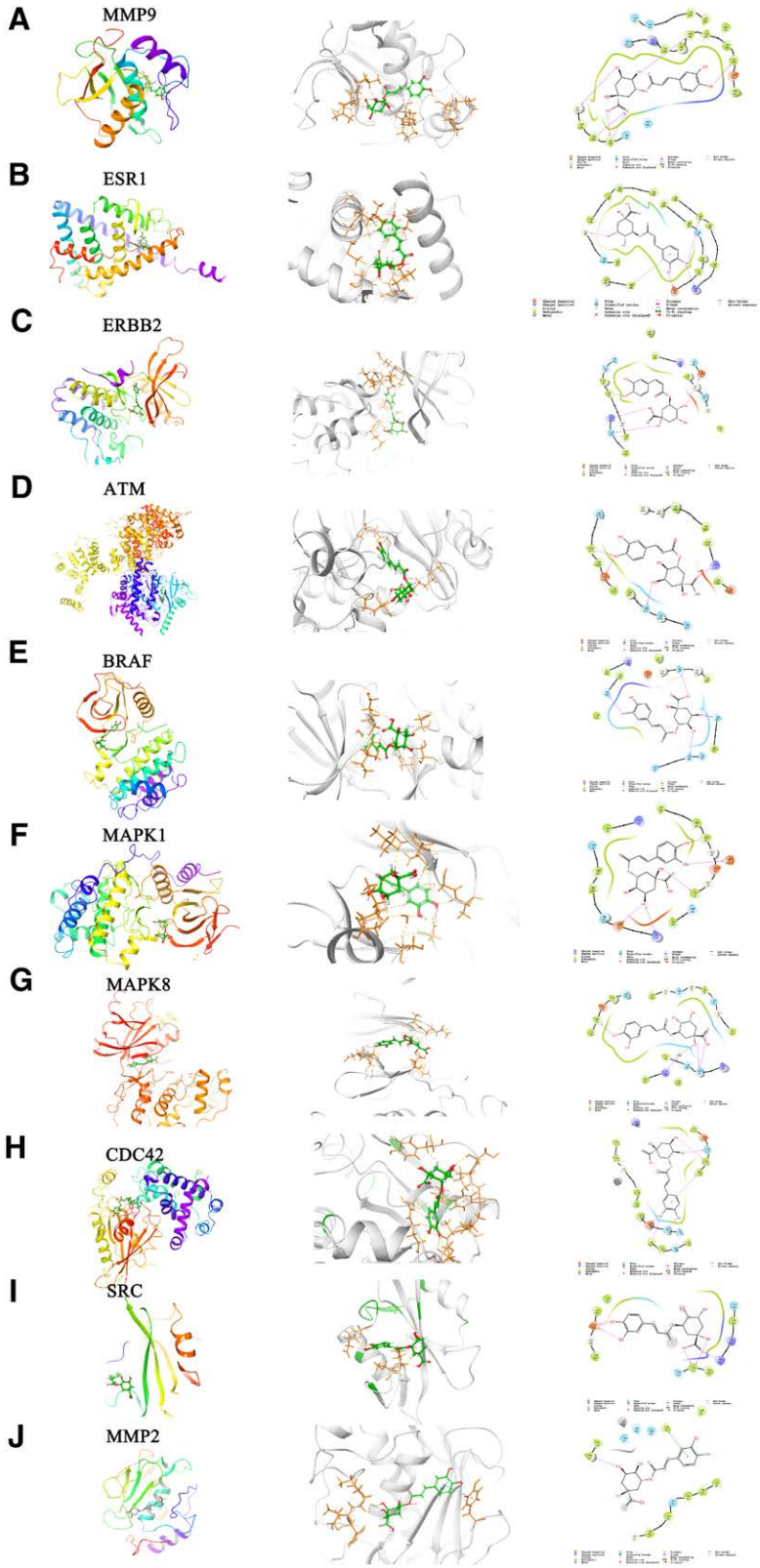

Figure 4. Molecular docking overall diagram–local diagram–detail diagram. The location of the binding pocket was determined according to the position of the small molecule in the complex structure of the target protein and the small molecule crystal. The docking algorithm was Maestro's default algorithm, and the number of cycles of the coordination capacity optimization for the docking was 100. ESR1 = estrogen receptor 1, ERBB2 = human epidermal growth factor receptor 2, MAPK1 = mitogen-activated protein kinase 1, MAPK8 = mitogen-activated protein kinase 8, MMP2 = matrix metallopeptidase 2, MMP9 = matrix metallopeptidase 9, SRC = SRC proto-oncogene.

Table 3

KEGG top 20 channels.

ID	Description	Gene ratio	Bg ratio	*P* value	*P* adjust	*q* value	Gene ID	Count
hsa01522	Endocrine resistance	13/21	98/8659	4.15E−21	6.85E−19	1.62E−19	MMP2/ERBB2/RAF1/CDK4/IGF1R/ESR1/PTK2/MAPK1/BRAF/MAPK8/ESR2/SRC/MMP9	13
hsa05219	Bladder cancer	45,556	41/8659	1.32E−16	1.09E−14	2.57E−15	MMP2/MMP1/ERBB2/RAF1/CDK4/MAPK1/BRAF/SRC/MMP9	9
hsa05205	Proteoglycans in cancer	45,647	205/8659	5.48E−15	3.02E−13	7.12E−14	MMP2/ERBB2/RAF1/IGF1R/ESR1/PTK2/FGFR1/MAPK1/BRAF/SRC/MMP9/CDC42	12
hsa05212	Pancreatic cancer	45,525	76/8659	4.48E−12	1.85E−10	4.37E−11	ERBB2/RAF1/CDK4/MAPK1/BRAF/MAPK8/CDC42/STAT1	8
hsa05224	Breast cancer	45,556	147/8659	2.26E−11	7.47E−10	1.76E−10	ERBB2/RAF1/CDK4/IGF1R/ESR1/FGFR1/MAPK1/BRAF/ESR2	9
hsa05215	Prostate cancer	45,525	97/8659	3.34E−11	9.19E−10	2.17E−10	ERBB2/RAF1/IGF1R/FGFR1/MAPK1/BRAF/CDK2/MMP9	8
hsa04917	Prolactin signaling pathway	45,494	70/8659	1.76E−10	4.16E−09	9.82E−10	RAF1/ESR1/MAPK1/MAPK8/ESR2/SRC/STAT1	7
hsa04510	Focal adhesion	45,556	203/8659	4.13E−10	8.52E−09	2.01E−09	ERBB2/RAF1/IGF1R/PTK2/MAPK1/BRAF/MAPK8/SRC/CDC42	9
hsa04012	ErbB signaling pathway	45,494	85/8659	7.11E−10	1.3E−08	3.08E−09	ERBB2/RAF1/PTK2/MAPK1/BRAF/MAPK8/SRC	7
hsa05161	Hepatitis B	45,525	162/8659	2.09E−09	3.45E−08	8.14E−09	RAF1/MAPK1/BRAF/CDK2/MAPK8/SRC/MMP9/STAT1	8
hsa05218	Melanoma	45,464	72/8659	1.31E−08	1.86E−07	4.39E−08	RAF1/CDK4/IGF1R/FGFR1/MAPK1/BRAF	6
hsa04926	Relaxin signaling pathway	45,494	129/8659	1.35E−08	1.86E−07	4.39E−08	MMP2/MMP1/RAF1/MAPK1/MAPK8/SRC/MMP9	7
hsa04068	FoxO signaling pathway	45,494	131/8659	1.51E−08	1.91E−07	4.51E−08	RAF1/IGF1R/ATM/MAPK1/BRAF/CDK2/MAPK8	7
hsa05417	Lipid and atherosclerosis	45,525	215/8659	1.96E−08	2.26E−07	5.34E−08	MMP1/PPARG/PTK2/MAPK1/MAPK8/SRC/MMP9/CDC42	8
hsa04915	Estrogen signaling pathway	45,494	137/8659	2.06E−08	2.26E−07	5.34E−08	MMP2/RAF1/ESR1/MAPK1/ESR2/SRC/MMP9	7
hsa01521	EGFR tyrosine kinase inhibitor resistance	45,464	79/8659	2.31E−08	2.39E−07	5.63E−08	ERBB2/RAF1/IGF1R/MAPK1/BRAF/SRC	6
hsa04520	Adherens junction	45,464	93/8659	6.22E−08	5.7E−07	1.35E−07	ERBB2/IGF1R/FGFR1/MAPK1/SRC/CDC42	6
hsa04912	GnRH signaling pathway	45,464	93/8659	6.22E−08	5.7E−07	1.35E−07	MMP2/RAF1/MAPK1/MAPK8/SRC/CDC42	6
hsa04933	AGE-RAGE signaling pathway in diabetic complications	45,464	100/8659	9.62E−08	8.35E−07	1.97E−07	MMP2/CDK4/MAPK1/MAPK8/CDC42/STAT1	6
hsa04914	Progesterone-mediated oocyte maturation	45,464	102/8659	1.08E−07	8.94E−07	2.11E−07	RAF1/IGF1R/MAPK1/BRAF/CDK2/MAPK8	6

KEGG = Kyoto Encyclopedia of Genes and Genomes.

biological process (BP), cellular component (CC), and molecular function (MF). Key pathways from KEGG analysis results were visualized using the Weisheng platform.

2.6. Kaplan–Meier analysis of core target

Due to the unavailability of OSCC-specific targets in the The Cancer Genome Atlas (TCGA) database, OSCC and core target information were compiled using R from the relevant gene target data for head and neck squamous cell carcinoma in TCGA for further analysis. The R packages "survival" and "survminer" analyzed survival and generated Kaplan–Meier curves. The study focused on Overall Survival with a Group Cutoff set at 0.5, thereby visualizing the survival analysis for core targets of chlorogenic acid treatment in OSCC.

2.7. Molecular docking

Molecular docking simulations were executed in Maestro (2018). Three-dimensional structures of protein complex crystals for the 10 core targets in chlorogenic acid treatment for OSCC were downloaded from the PDB database. The small molecule structure of chlorogenic acid was sourced from the PubChem database and subjected to energy minimization in Chem3D to select the optimal conformation. These target complex protein crystals and chlorogenic acid small molecules were then processed in Maestro for docking simulation, yielding molecular docking data.

2.8. Statistical analysis

Survival differences among groups were assessed using the log-rank test and depicted via Kaplan–Meier (KM) survival maps. All *P* values were derived from 2-sided statistics, with a *P* value < .05 deemed statistically significant. Bioinformatics data were analyzed using R × 64 4.2.2, Cytoscape 3.9.1, the GEPIA online platform, and the Microbioinformatics online mapping tool.

3. Results

3.1. Chlorogenic acid and potential targets for oral squamous cell carcinoma (OSCC)

Two hundred potential targets of chlorogenic acid were identified through the Therapeutic Target Database, ChEMBL Database, HERB database, PharmMapper database, and SwissTargetPrediction screening (see Table S2, Supplemental Digital Content, http://links.lww.com/MD/N777, which explains chlorogenic acid related targets). These targets include estrogen receptor 1 (*ESR1*), human epidermal growth factor receptor 2 (*ErbB2*), and matrix metallopeptidase 2 (*MMP2*), among others. The "compound - drug prediction target" network diagram (Fig. 1A) visually represents potential targets for chlorogenic acid-binding. OSCC-related genes were sourced from OMIM and GeneCards using "oral squamous cell carcinoma" as the search keyword. The OMIM search yielded 300 relevant targets, while GeneCards provided 5490 relevant targets. From these, targets with correlation scores above 50 were selected as relevant to OSCC (Fig. 1B). After combining these datasets and removing duplicates, 430 OSCC potential targets were identified as potential disease targets.

3.2. Screening of core targets for chlorogenic acid treatment of OSCC

Twenty three intersecting genes between chlorogenic acid and OSCC were identified as potential targets for chlorogenic acid

Table 4

The first 20 paths of each part of GO.

Ontology	ID	Description	Gene ratio	Bg ratio	*P* value	*P* adjust	*q* value	Gene ID	Count
BP	GO:0009612	Response to mechanical stimulus	45,527	211/18,903	8.96E−11	1.53E−07	6.98E−08	MMP2/RAF1/IGF1R/PTK2/DDR2/MAPK8/SRC/STAT1	8
BP	GO:0048660	Regulation of smooth muscle cell proliferation	45,496	175/18,903	1.12E−09	6.67E−07	3.04E−07	MMP2/IGF1R/PPARG/DDR2/SRC/MMP9/STAT1	7
BP	GO:0048659	Smooth muscle cell proliferation	45,496	179/18,903	1.31E−09	6.67E−07	3.04E−07	MMP2/IGF1R/PPARG/DDR2/SRC/MMP9/STAT1	7
BP	GO:0048661	Positive regulation of smooth muscle cell proliferation	45,466	98/18,903	1.56E−09	6.67E−07	3.04E−07	MMP2/IGF1R/DDR2/SRC/MMP9/STAT1	6
BP	GO:0000302	Response to reactive oxygen species	45,496	204/18,903	3.26E−09	1.11E−06	5.07E−07	MMP2/MAPK1/DDR2/MAPK8/SRC/MMP9/STAT1	7
BP	GO:0046777	Protein autophosphorylation	45,496	226/18,903	6.63E−09	1.75E−06	7.96E−07	ERBB2/IGF1R/PTK2/FGFR1/ATM/DDR2/SRC	7
BP	GO:0038127	ERBB signaling pathway	45,466	126/18,903	7.16E−09	1.75E−06	7.96E−07	ERBB2/PTK2/MAPK1/BRAF/SRC/MMP9	6
BP	GO:0033002	Muscle cell proliferation	45,496	247/18,903	1.23E−08	2.62E−06	1.19E−06	MMP2/IGF1R/PPARG/DDR2/SRC/MMP9/STAT1	7
BP	GO:0034614	Cellular response to reactive oxygen species	45,466	150/18,903	2.04E−08	3.87E−06	1.77E−06	MMP2/MAPK1/DDR2/MAPK8/SRC/MMP9	6
BP	GO:0071375	Cellular response to peptide hormone stimulus	45,496	306/18,903	5.34E−08	8.38E−06	3.82E−06	CDK4/IGF1R/PPARG/PTK2/DDR2/SRC/STAT1	7
BP	GO:0050673	Epithelial cell proliferation	45,527	481/18,903	5.81E−08	8.38E−06	3.82E−06	ERBB2/CDK4/ESR1/PPARG/FGFR1/MAPK1/CDC42/STAT1	8
BP	GO:0018105	Peptidyl-serine phosphorylation	45,496	313/18,903	6.23E−08	8.38E−06	3.82E−06	RAF1/ATM/MAPK1/BRAF/CDK2/MAPK8/SRC	7
BP	GO:0001667	Ameboidal-type cell migration	45,527	492/18,903	6.92E−08	8.38E−06	3.82E−06	PPARG/PTK2/FGFR1/DDR2/BRAF/SRC/MMP9/CDC42	8
BP	GO:0033674	Positive regulation of kinase activity	45,527	496/18,903	7.36E−08	8.38E−06	3.82E−06	ERBB2/IGF1R/PTK2/FGFR1/DDR2/ROS1/SRC/CDC42	8
BP	GO:0043410	Positive regulation of MAPK cascade	45,527	496/18,903	7.36E−08	8.38E−06	3.82E−06	ERBB2/RAF1/IGF1R/FGFR1/DDR2/BRAF/SRC/CDC42	8
BP	GO:1904705	Regulation of vascular associated smooth muscle cell proliferation	45,435	93/18,903	8.11E−08	8.66E−06	3.95E−06	MMP2/PPARG/DDR2/SRC/MMP9	5
BP	GO:1990874	Vascular associated smooth muscle cell proliferation	45,435	95/18,903	9.03E−08	8.84E−06	4.03E−06	MMP2/PPARG/DDR2/SRC/MMP9	5
BP	GO:0018209	Peptidyl-serine modification	45,496	332/18,903	9.32E−08	8.84E−06	4.03E−06	RAF1/ATM/MAPK1/BRAF/CDK2/MAPK8/SRC	7
BP	GO:0062197	Cellular response to chemical stress	45,496	345/18,903	1.21E−07	1.09E−05	4.96E−06	MMP2/ATM/MAPK1/DDR2/MAPK8/SRC/MMP9	7
BP	GO:0071392	Cellular response to estradiol stimulus	45,405	40/18,903	1.48E−07	1.26E−05	5.76E−06	MMP2/IGF1R/ESR1/ESR2	4
CC	GO:0005925	Focal adhesion	45,435	422/19,869	.000104	.004315	0.00288	PTK2/MAPK1/DDR2/SRC/CDC42	5
CC	GO:0005901	Caveola	45,374	82/19,869	.000113	.004315	0.00288	IGF1R/MAPK1/SRC	3
CC	GO:0030055	Cell-substrate junction	45,435	432/19,869	.000116	.004315	0.00288	PTK2/MAPK1/DDR2/SRC/CDC42	5
CC	GO:0031143	Pseudopodium	45,345	18/19,869	.000194	.00543	0.003623	RAF1/MAPK1	2
CC	GO:0044853	Plasma membrane raft	45,374	113/19,869	.000292	.00654	0.004364	IGF1R/MAPK1/SRC	3
CC	GO:1902911	Protein kinase complex	45,374	136/19,869	.000502	.00938	0.006259	CDK4/IGF1R/CDK2	3
CC	GO:0000307	Cyclin-dependent protein kinase holoenzyme complex	45,345	50/19,869	.001518	.024288	0.016207	CDK4/CDK2	2
CC	GO:0061695	Transferase complex, transferring phosphorus-containing groups	45,374	295/19,869	.004604	.062395	0.041635	CDK4/IGF1R/CDK2	3
CC	GO:0031234	Extrinsic component of cytoplasmic side of plasma membrane	45,345	99/19,869	.005808	.062395	0.041635	PTK2/SRC	2
CC	GO:0045121	Membrane raft	45,374	326/19,869	.006076	.062395	0.041635	IGF1R/MAPK1/SRC	3
CC	GO:0098857	Membrane microdomain	45,374	327/19,869	.006128	.062395	0.041635	IGF1R/MAPK1/SRC	3
CC	GO:0030175	Filopodium	45,345	108/19,869	.006874	.064161	0.042814	SRC/CDC42	2
CC	GO:1902554	Serine/threonine protein kinase complex	45,345	122/19,869	.008696	.071634	0.047801	CDK4/CDK2	2
CC	GO:1904813	Ficolin-1-rich granule lumen	45,345	124/19,869	.008972	.071634	0.047801	MAPK1/MMP9	2
CC	GO:0000805	X chromosome	45,314	10/19,869	.011518	.071634	0.047801	CDK2	1
CC	GO:0099091	Postsynaptic specialization, intracellular component	45,314	10/19,869	.011518	.071634	0.047801	SRC	1
CC	GO:0005819	Spindle	45,374	426/19,869	.012604	.071634	0.047801	ATM/MAPK1/CDC42	3
CC	GO:0017119	Golgi transport complex	45,314	11/19,869	.012663	.071634	0.047801	CDC42	1
CC	GO:0097550	Transcription preinitiation complex	45,314	11/19,869	.012663	.071634	0.047801	ESR1	1
CC	GO:0045177	Apical part of cell	45,374	435/19,869	.013332	.071634	0.047801	ERBB2/DDR2/CDC42	3
MF	GO:0004713	Protein tyrosine kinase activity	45,496	138/18,432	2.51E−10	3.76E−08	1.64E−08	ERBB2/IGF1R/PTK2/FGFR1/DDR2/ROS1/SRC	
MF	GO:0004714	Transmembrane receptor protein tyrosine kinase activity	45,435	60/18,432	9.92E−09	7.44E−07	3.24E−07	ERBB2/IGF1R/FGFR1/DDR2/ROS1	
MF	GO:0019199	Transmembrane receptor protein kinase activity	45,435	79/18,432	4.03E−08	2.01E−06	8.77E−07	ERBB2/IGF1R/FGFR1/DDR2/ROS1	
MF	GO:0019902	Phosphatase binding	45,466	195/18,432	1.13E−07	4.23E−06	1.84E−06	ERBB2/PTK2/MAPK1/ROS1/MAPK8/STAT1	
MF	GO:0106310	Protein serine kinase activity	45,496	363/18,432	2.03E−07	6.08E−06	2.64E−06	RAF1/CDK4/ATM/MAPK1/BRAF/CDK2/MAPK8	
MF	GO:0004674	Protein serine/threonine kinase activity	45,496	430/18,432	6.36E−07	1.59E−05	6.91E−06	RAF1/CDK4/ATM/MAPK1/BRAF/CDK2/MAPK8	
MF	GO:0019903	Protein phosphatase binding	45,435	149/18,432	9.66E−07	2.07E−05	9E−06	ERBB2/PTK2/ROS1/MAPK8/STAT1	
MF	GO:0016922	Nuclear receptor binding	45,405	139/18,432	2.45E−05	.00046	0.0002	ESR1/PPARG/SRC/STAT1	

(*Continued*)

Table 4
(Continued)

Ontology	ID	Description	Gene ratio	Bg ratio	*P* value	*P* adjust	*q* value	Gene ID	Count
MF	GO:0004879	Nuclear receptor activity	45,374	52/18,432	3.6E−05	.000541	0.000235	ESR1/PPARG/ESR2	
MF	GO:0098531	Ligand-activated transcription factor activity	45,374	52/18,432	3.6E−05	.000541	0.000235	ESR1/PPARG/ESR2	
MF	GO:0008353	RNA polymerase II CTD heptapeptide repeat kinase activity	45,345	13/18,432	.000115	.001571	0.000684	CDK4/MAPK1	
MF	GO:0004707	MAP kinase activity	45,345	16/18,432	.000177	.002211	0.000962	MAPK1/MAPK8	
MF	GO:0004708	MAP kinase kinase activity	45,345	18/18,432	.000225	.002598	0.00113	MAPK1/BRAF	
MF	GO:0035173	Histone kinase activity	45,345	20/18,432	.000279	.002991	0.001301	ATM/CDK2	
MF	GO:0001221	Transcription coregulator binding	45,374	109/18,432	.000327	.003123	0.001359	ESR1/PPARG/STAT1	
MF	GO:0005158	Insulin receptor binding	45,345	22/18,432	.000339	.003123	0.001359	IGF1R/SRC	
MF	GO:0004222	Metalloendopeptidase activity	45,374	112/18,432	.000354	.003123	0.001359	MMP2/MMP1/MMP9	
MF	GO:0003707	Nuclear steroid receptor activity	45,345	24/18,432	.000404	.003369	0.001466	ESR1/ESR2	
MF	GO:0004709	MAP kinase kinase kinase activity	45,345	27/18,432	.000513	.004039	0.001758	RAF1/BRAF	
MF	GO:0019838	Growth factor binding	45,374	132/18,432	.000573	.004039	0.001758	ERBB2/IGF1R/FGFR1	

BP = biological process, CC = cell component, GO = Gene Ontology, MAPK = mitogen-activated protein kinase, MF = molecular function.

treatment of OSCC (Fig. 2A). These overlapping genes were input into the STRING database to construct the PPI network (Fig. 2B). The PPI data were analyzed in Cytoscape to identify 10 core targets for chlorogenic acid treatment of OSCC based on the network's topological characteristics (Table 1, Fig. 2C,D).

3.3. Survival curve analysis

Core target data from TCGA were analyzed using R language for survival analysis and curve generation. The resulting figure (Fig. 3A) indicates that, except *ATM* and *BRAF*, other genes significantly influence patient survival times, including *ESR1, MMP2, MMP9, SRC, MAPK8, MAPK1, CDC42, and ERBB2*. The analysis demonstrates that the downregulation of these core target genes is advantageous for patient survival.

3.4. Molecular docking

To assess the potential of chlorogenic acid in treating OSCC, we integrated the 10 core target proteins identified previously with small drug molecules into Maestro, simulating the binding capabilities between the drugs and targets through chemical analysis. The docking score's absolute value reflects the likelihood of interaction, with values below −5 indicating binding solid potential. The docking scores for chlorogenic acid and the target proteins were below −5 (Table 2, Fig. 4), with *MMP9* demonstrating the highest docking score. The root mean square deviation indicates the reliability of the docking results. Except for *MAPK1*, all the docking results are <3, and the root mean square deviation values of *MMP2, ATM* and *BRAF* are <2, indicating strong reliability of the docking results (Table 3).

3.5. GO analysis and KEGG analysis (Gene Ontology analysis and Kyoto Encyclopedia of Genes and Genomes pathway enrichment analysis)

The molecular mechanisms underlying chlorogenic acid's therapeutic effects on OSCC were explored through the computational analysis of cross-gene data using the R package "clusterProfiler." The KEGG analysis revealed 128 pathways, with the foremost 20 and 15 presented in Table 4 and Figure 5A, respectively. Pathways pertinent to cell growth, migration, adhesion, cell cycle, and endocrine resistance were significantly implicated in OSCC. The ErbB pathway, Proteoglycans in the cancer pathway, and Endocrine resistance pathway mechanisms are depicted in Figure 5B–D. These diagrams highlight the critical roles of the ERK and JNK branches of the MAPK signaling pathway, closely tied to cell growth, migration, and adhesion. GO analysis, categorized into BP, CC, and MF sections, identified 965 BP items, 41 CC items, and 88 MF items, with the top 20 of each displayed in Table 5 and Figure 5E. BP is predominantly related to immune processes.

4. Discussion

OSCC is among the most prevalent malignancies in the head and neck region and is characterized by high invasiveness and heterogeneity.[16] Despite continuous advancements in treatment methods, the complexity of its pathogenesis and ambiguous diagnostic criteria limits the efficacy of therapeutic drugs.[17] Chlorogenic acid, which is extensively used in cancer therapy, has seen limited research in the context of OSCC.[18]

In this study, we identified 200 potential targets of chlorogenic acid and 430 gene targets related to OSCC for further analysis. Through Venn diagram analysis of these datasets, we pinpointed crucial drug treatment targets and conducted

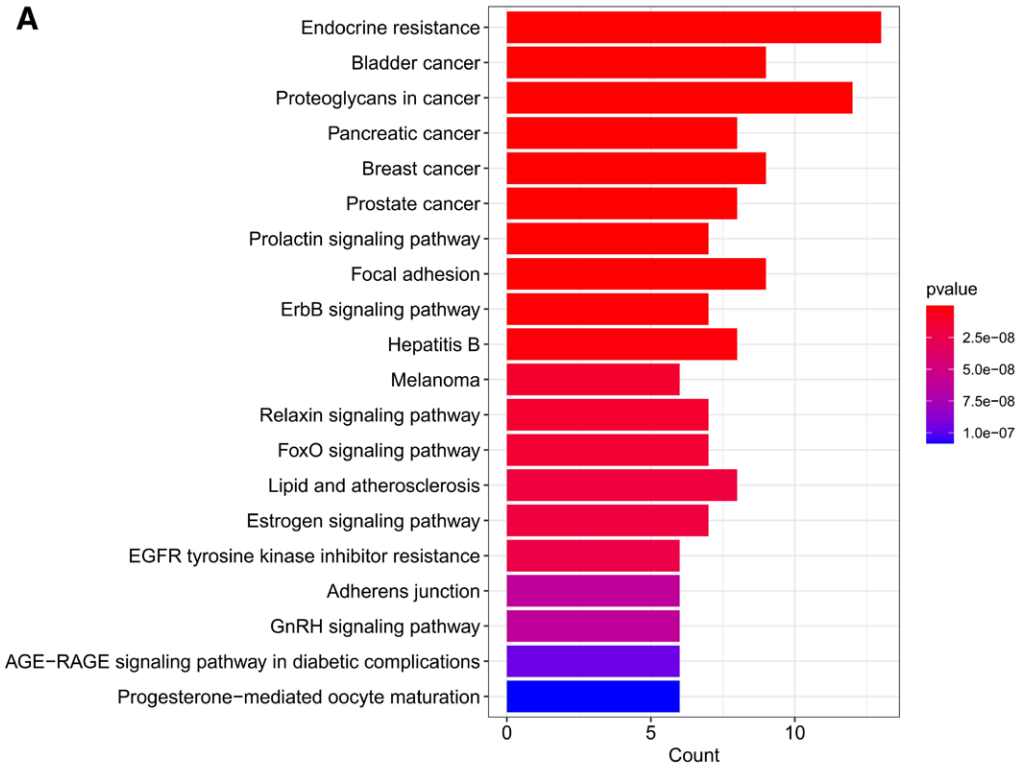

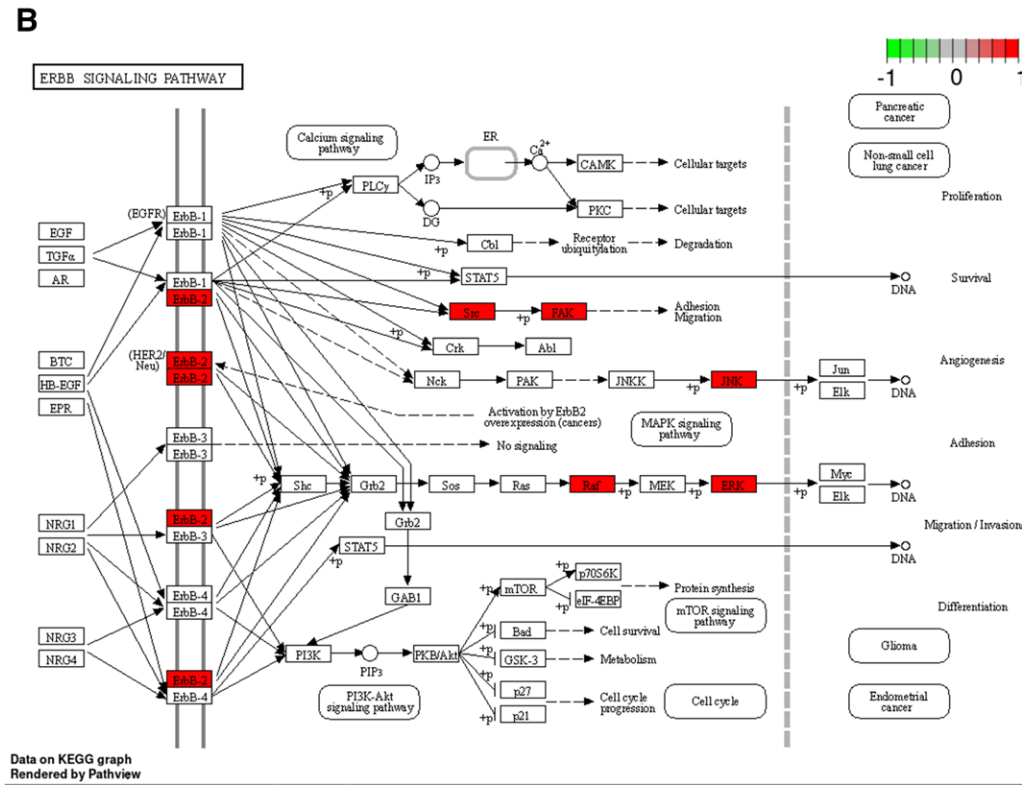

Figure 5. (A) KEGG enrichment analysis of targets for chlorogenic acid treatment of diseases, with the top 15 important items shown. (B) ErbB pathway visualization with red indicating key targets for chlorogenic acid treatment of OSCC. (C) Visualization of Proteoglycans in cancer pathway, with red indicating key targets for chlorogenic acid treatment of OSCC. (D) Visualization of the Endocrine resistance pathway, with red indicating key targets for chlorogenic acid treatment of OSCC. (E) The key first 15 entries in the BP, CC, and MF sections of GO. BP = biological process, CC = cell component, GO = Gene Ontology, KEGG = Kyoto Encyclopedia of Genes and Genomes, MF = molecular function, OSCC = oral squamous cell carcinoma.

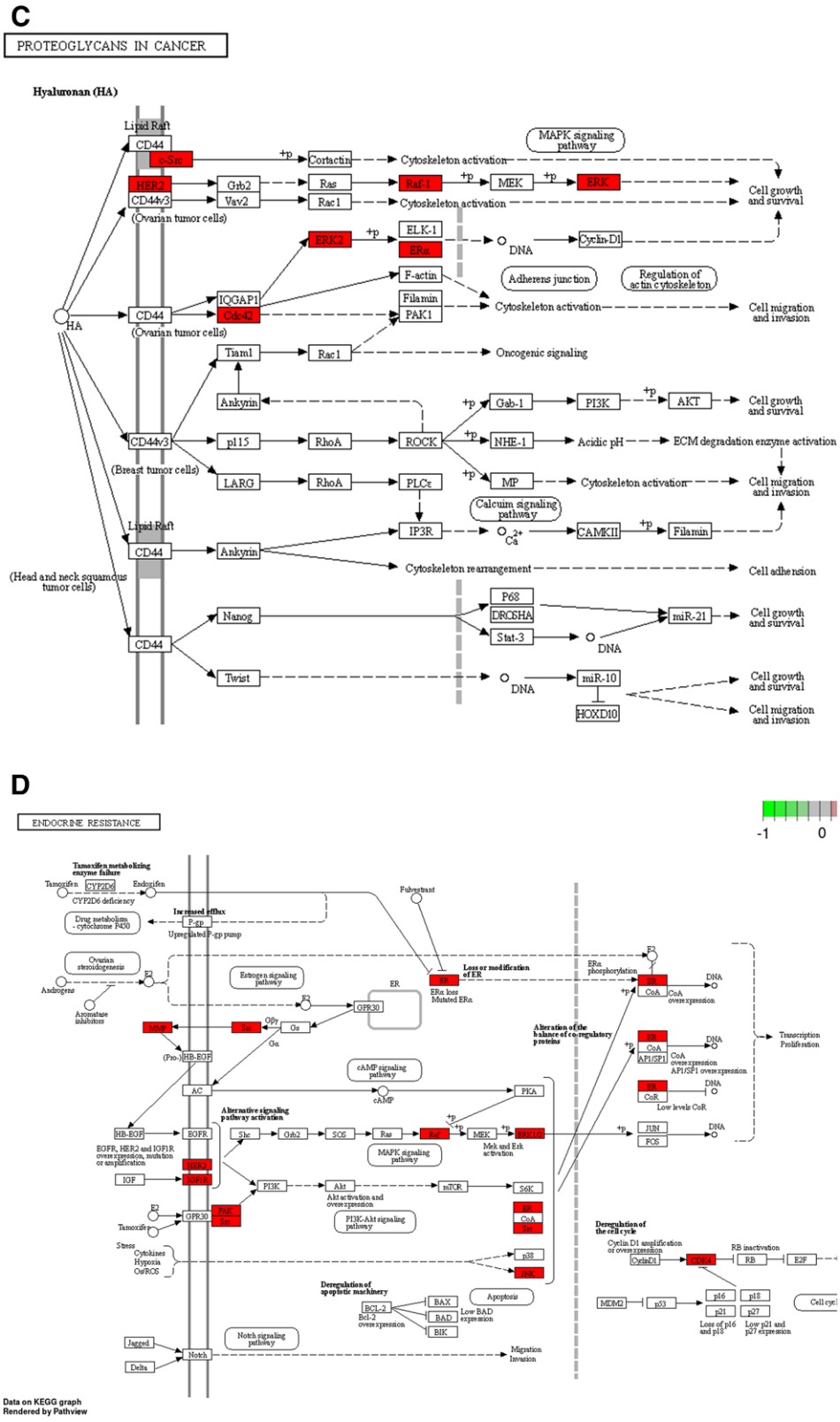

Figure 5. Continued

KEGG and GO analyses to determine vital molecular mechanisms. Network analysis of essential genes facilitated the calculation of core targets, which were then validated via molecular docking and Kaplan–Meier (KM) curve analysis (Fig. 6). The core targets identified include *ESR1*, *MMP2*, *MMP9*, *SRC*, *MAPK8 (JNK1)*, *MAPK1*, *CDC42*, *ERBB2*, *ATM*, *and BRAF*, totaling ten data points. The experimental process is shown in Figure 6.

KEGG analysis indicated that treatment with chlorogenic acid may affect cell growth, adhesion, migration, and the cell cycle, with most targets involved in the *ERK* and *JNK* pathways within *MAPK*. Abnormal activation of proteins in the

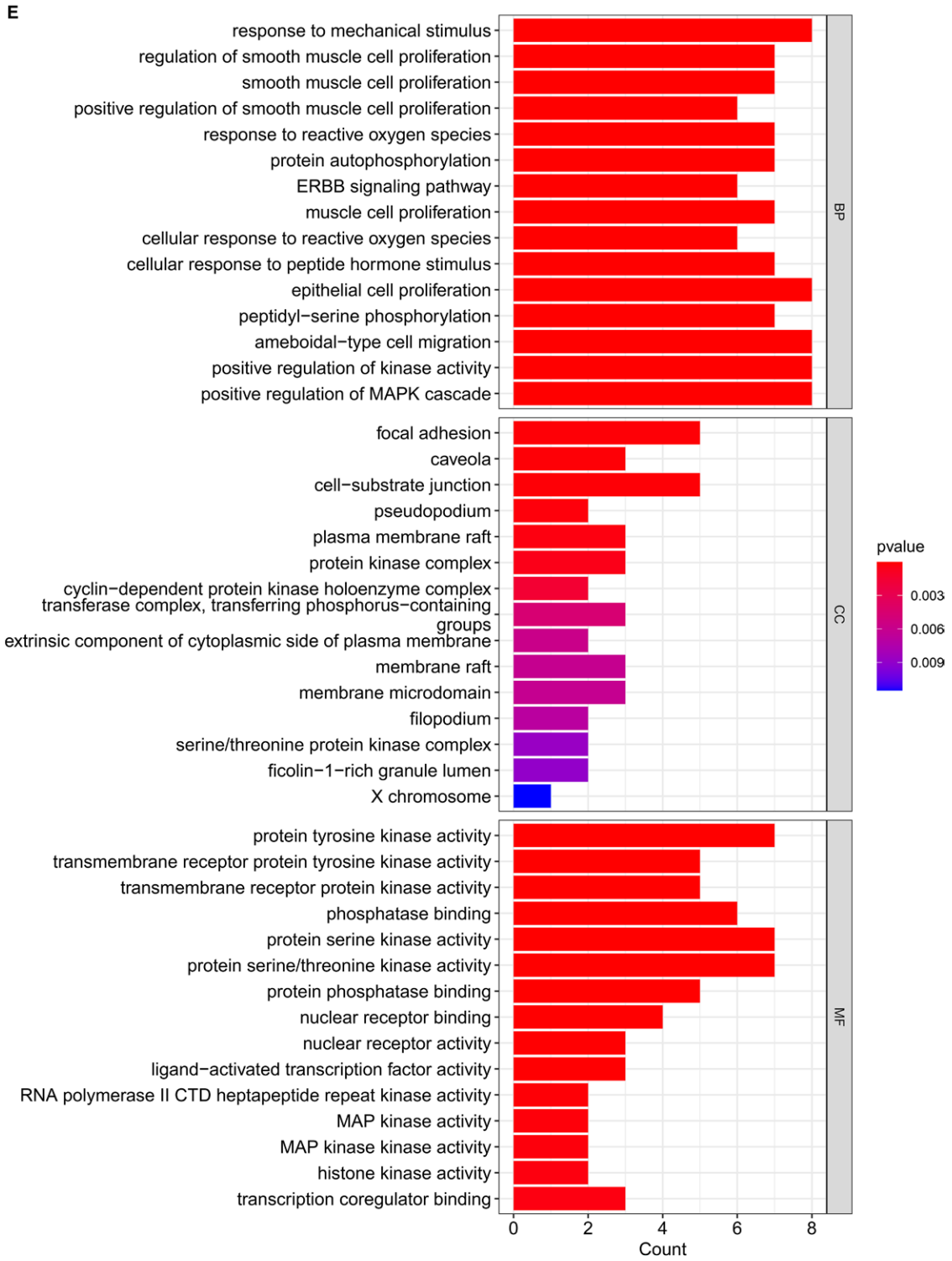

Figure 5. Continued

MAPK pathway is a critical factor in many cancers, and targeting this pathway may be a viable tumor treatment strategy.[19,20] *ERK* primarily influences cell growth, migration, and the cell cycle and receives upstream signals from *Ras/Raf* proteins.[21,22] The *JNK* pathway is also associated with inflammation, apoptosis, and cell growth. Core targets such as *ERBB2, SRC, MAPK1 (ERK2), BRAF,* and *CDC42* in the *ErbB* and proteoglycan pathways in cancer are implicated in cell growth, migration, and adhesion via the *ERK* pathway. The *ERK* pathway has gained significant attention in OSCC research. The overexpression of growth differentiation factor 15 enhances *ErbB2* phosphorylation, triggering downstream *AKT* and *ERK* signaling pathways promoting OSCC cell proliferation.[23] The combined action of p63 and the *MEK/ERK-MAPK* pathway synergistically induces *ARL4C* expression, thereby promoting the growth and proliferation of OSCC tumor cells.[24] Semilicoisoflavone B downregulates *MAPK* and *Ras/Raf/MEK* signaling and concurrently induces reactive oxygen species production to trigger OSCC cell apoptosis.[25] Machilin D impedes the *FAK/Src* and *MAPK* pathways,

Table 5

The first 20 paths of each part of GO.

Ontology	ID	Description	Gene ratio	Bg ratio	*P* value	*P* adjust	*q* value	Gene ID	Count
BP	GO:0009612	Response to mechanical stimulus	45,527	211/18,903	8.96E−11	1.53E−07	6.98E−08	MMP2/RAF1/IGF1R/PTK2/DDR2/MAPK8/SRC/STAT1	8
BP	GO:0048660	Regulation of smooth muscle cell proliferation	45,496	175/18,903	1.12E−09	6.67E−07	3.04E−07	MMP2/IGF1R/PPARG/DDR2/SRC/MMP9/STAT1	7
BP	GO:0048659	Smooth muscle cell proliferation	45,496	179/18,903	1.31E−09	6.67E−07	3.04E−07	MMP2/IGF1R/PPARG/DDR2/SRC/MMP9/STAT1	7
BP	GO:0048661	Positive regulation of smooth muscle cell proliferation	45,466	98/18,903	1.56E−09	6.67E−07	3.04E−07	MMP2/IGF1R/DDR2/SRC/MMP9/STAT1	6
BP	GO:0000302	Response to reactive oxygen species	45,496	204/18,903	3.26E−09	1.11E−06	5.07E−07	MMP2/MAPK1/DDR2/MAPK8/SRC/MMP9/STAT1	7
BP	GO:0046777	Protein autophosphorylation	45,496	226/18,903	6.63E−09	1.75E−06	7.96E−07	ERBB2/IGF1R/PTK2/FGFR1/ATM/DDR2/SRC	7
BP	GO:0038127	ERBB signaling pathway	45,466	126/18,903	7.16E−09	1.75E−06	7.96E−07	ERBB2/PTK2/MAPK1/BRAF/SRC/MMP9	6
BP	GO:0033002	Muscle cell proliferation	45,496	247/18,903	1.23E−08	2.62E−06	1.19E−06	MMP2/IGF1R/PPARG/DDR2/SRC/MMP9/STAT1	7
BP	GO:0034614	Cellular response to reactive oxygen species	45,466	150/18,903	2.04E−08	3.87E−06	1.77E−06	MMP2/MAPK1/DDR2/MAPK8/SRC/MMP9	6
BP	GO:0071375	Cellular response to peptide hormone stimulus	45,496	306/18,903	5.34E−08	8.38E−06	3.82E−06	CDK4/IGF1R/PPARG/PTK2/DDR2/SRC/STAT1	7
BP	GO:0050673	Epithelial cell proliferation	45,527	481/18,903	5.81E−08	8.38E−06	3.82E−06	ERBB2/CDK4/ESR1/PPARG/FGFR1/MAPK1/CDC42/STAT1	8
BP	GO:0018105	Peptidyl-serine phosphorylation	45,496	313/18,903	6.23E−08	8.38E−06	3.82E−06	RAF1/ATM/MAPK1/BRAF/CDK2/MAPK8/SRC	7
BP	GO:0001667	Ameboidal-type cell migration	45,527	492/18,903	6.92E−08	8.38E−06	3.82E−06	PPARG/PTK2/FGFR1/DDR2/BRAF/SRC/MMP9/CDC42	8
BP	GO:0033674	Positive regulation of kinase activity	45,527	496/18,903	7.36E−08	8.38E−06	3.82E−06	ERBB2/IGF1R/PTK2/FGFR1/DDR2/ROS1/SRC/CDC42	8
BP	GO:0043410	Positive regulation of MAPK cascade	45,527	496/18,903	7.36E−08	8.38E−06	3.82E−06	ERBB2/RAF1/IGF1R/FGFR1/DDR2/BRAF/SRC/CDC42	8
BP	GO:1904705	Regulation of vascular associated smooth muscle cell proliferation	45,435	93/18,903	8.11E−08	8.66E−06	3.95E−06	MMP2/PPARG/DDR2/SRC/MMP9	5
BP	GO:1990874	Vascular associated smooth muscle cell proliferation	45,435	95/18,903	9.03E−08	8.84E−06	4.03E−06	MMP2/PPARG/DDR2/SRC/MMP9	5
BP	GO:0018209	Peptidyl-serine modification	45,496	332/18,903	9.32E−08	8.84E−06	4.03E−06	RAF1/ATM/MAPK1/BRAF/CDK2/MAPK8/SRC	7
BP	GO:0062197	Cellular response to chemical stress	45,496	345/18,903	1.21E−07	1.09E−05	4.96E−06	MMP2/ATM/MAPK1/DDR2/MAPK8/SRC/MMP9	7
BP	GO:0071392	Cellular response to estradiol stimulus	45,405	40/18,903	1.48E−07	1.26E−05	5.76E−06	MMP2/IGF1R/ESR1/ESR2	4
CC	GO:0005925	Focal adhesion	45,435	422/19,869	.000104	.004315	0.00288	PTK2/MAPK1/DDR2/SRC/CDC42	5
CC	GO:0005901	Caveola	45,374	82/19,869	.000113	.004315	0.00288	IGF1R/MAPK1/SRC	3
CC	GO:0030055	Cell-substrate junction	45,435	432/19,869	.000116	.004315	0.00288	PTK2/MAPK1/DDR2/SRC/CDC42	5
CC	GO:0031143	Pseudopodium	45,345	18/19,869	.000194	.00543	0.003623	RAF1/MAPK1	2
CC	GO:0044853	Plasma membrane raft	45,374	113/19,869	.000292	.00654	0.004364	IGF1R/MAPK1/SRC	3
CC	GO:1902911	Protein kinase complex	45,374	136/19,869	.000502	.00938	0.006259	CDK4/IGF1R/CDK2	3
CC	GO:0000307	Cyclin-dependent protein kinase holoenzyme complex	45,345	50/19,869	.001518	.024288	0.016207	CDK4/CDK2	2
CC	GO:0061695	Transferase complex, transferring phosphorus-containing groups	45,374	295/19,869	.004604	.062395	0.041635	CDK4/IGF1R/CDK2	3
CC	GO:0031234	Extrinsic component of cytoplasmic side of plasma membrane	45,345	99/19,869	.005808	.062395	0.041635	PTK2/SRC	2
CC	GO:0045121	Membrane raft	45,374	326/19,869	.006076	.062395	0.041635	IGF1R/MAPK1/SRC	3
CC	GO:0098857	Membrane microdomain	45,374	327/19869	.006128	.062395	0.041635	IGF1R/MAPK1/SRC	3
CC	GO:0030175	Filopodium	45,345	108/19,869	.006874	.064161	0.042814	SRC/CDC42	2
CC	GO:1902554	Serine/threonine protein kinase complex	45,345	122/19,869	.008696	.071634	0.047801	CDK4/CDK2	2
CC	GO:1904813	Ficolin-1-rich granule lumen	45,345	124/19,869	.008972	.071634	0.047801	MAPK1/MMP9	2
CC	GO:0000805	X chromosome	45,314	10/19,869	.011518	.071634	0.047801	CDK2	1
CC	GO:0099091	Postsynaptic specialization, intracellular component	45,314	10/19,869	.011518	.071634	0.047801	SRC	1
CC	GO:0005819	Spindle	45,374	426/19,869	.012604	.071634	0.047801	ATM/MAPK1/CDC42	3
CC	GO:0017119	Golgi transport complex	45,314	11/19,869	.012663	.071634	0.047801	CDC42	1
CC	GO:0097550	Transcription preinitiation complex	45,314	11/19,869	.012663	.071634	0.047801	ESR1	1
CC	GO:0045177	Apical part of cell	45,374	435/19,869	.013332	.071634	0.047801	ERBB2/DDR2/CDC42	3
MF	GO:0004713	Protein tyrosine kinase activity	45,496	138/18,432	2.51E−10	3.76E−08	1.64E−08	ERBB2/IGF1R/PTK2/FGFR1/DDR2/ROS1/SRC	
MF	GO:0004714	Transmembrane receptor protein tyrosine kinase activity	45,435	60/18,432	9.92E−09	7.44E−07	3.24E−07	ERBB2/IGF1R/FGFR1/DDR2/ROS1	
MF	GO:0019199	Transmembrane receptor protein kinase activity	45,435	79/18,432	4.03E−08	2.01E−06	8.77E−07	ERBB2/IGF1R/FGFR1/DDR2/ROS1	
MF	GO:0019902	Phosphatase binding	45,466	195/18,432	1.13E−07	4.23E−06	1.84E−06	ERBB2/PTK2/MAPK1/ROS1/MAPK8/STAT1	
MF	GO:0106310	Protein serine kinase activity	45,496	363/18,432	2.03E−07	6.08E−06	2.64E−06	RAF1/CDK4/ATM/MAPK1/BRAF/CDK2/MAPK8	
MF	GO:0004674	Protein serine/threonine kinase activity	45,496	430/18,432	6.36E−07	1.59E−05	6.91E−06	RAF1/CDK4/ATM/MAPK1/BRAF/CDK2/MAPK8	
MF	GO:0019903	Protein phosphatase binding	45,435	149/18,432	9.66E−07	2.07E−05	9E−06	ERBB2/PTK2/ROS1/MAPK8/STAT1	
MF	GO:0016922	Nuclear receptor binding	45,405	139/18,432	2.45E−05	.00046	0.0002	ESR1/PPARG/SRC/STAT1	

(*Continued*)

Table 5
(Continued)

Ontology	ID	Description	Gene ratio	Bg ratio	*P* value	*P* adjust	*q* value	Gene ID	Count
MF	GO:0004879	Nuclear receptor activity	45,374	52/18,432	3.6E−05	.000541	0.000235	ESR1/PPARG/ESR2	
MF	GO:0098531	Ligand-activated transcription factor activity	45,374	52/18,432	3.6E−05	.000541	0.000235	ESR1/PPARG/ESR2	
MF	GO:0008353	RNA polymerase II CTD heptapeptide repeat kinase activity	45,345	13/18,432	.000115	.001571	0.000684	CDK4/MAPK1	
MF	GO:0004707	MAP kinase activity	45,345	16/18,432	.000177	.002211	0.000962	MAPK1/MAPK8	
MF	GO:0004708	MAP kinase kinase activity	45,345	18/18,432	.000225	.002598	0.00113	MAPK1/BRAF	
MF	GO:0035173	Histone kinase activity	45,345	20/18,432	.000279	.002991	0.001301	ATM/CDK2	
MF	GO:0001221	Transcription coregulator binding	45,374	109/18,432	.000327	.003123	0.001359	ESR1/PPARG/STAT1	
MF	GO:0005158	Insulin receptor binding	45,345	22/18,432	.000339	.003123	0.001359	IGF1R/SRC	
MF	GO:0004222	Metalloendopeptidase activity	45,374	112/18,432	.000354	.003123	0.001359	MMP2/MMP1/MMP9	
MF	GO:0003707	Nuclear steroid receptor activity	45,345	24/18,432	.000404	.003369	0.001466	ESR1/ESR2	
MF	GO:0004709	MAP kinase kinase kinase activity	45,345	27/18,432	.000513	.004039	0.001758	RAF1/BRAF	
MF	GO:0019838	Growth factor binding	45,374	132/18,432	.000573	.004039	0.001758	ERBB2/IGF1R/FGFR1	

BP = biological process, CC = cell component, GO = Gene Ontology, MAPK = mitogen-activated protein kinase, MF = molecular function.

reducing the adhesion, migration, and invasion of OSCC cells, leading to apoptotic cell death.[26] 7-Epitaxol reduces *ERK1/2* phosphorylation and elevates the expression of OSCC cell apoptosis and autophagy marker proteins (cleaved-poly ADP-ribose polymerase and microtubule-associated protein 1 light chain 3-I/II).[27] The expression of *BRAF*-activated long non-coding RNA is positively correlated with *MAPK* signaling pathway-associated proteins (*p-erk, p-akt,* and *p-38*).[28] Its suppression notably hinders OSCC cell proliferation, migration, and invasion, whereas overexpression has the opposite effect. The galectin-1 inhibitor OTX008 decreased OSCC cell viability in a dose-dependent manner through the *MAPK/ERK* pathway.[29] Isorhamnetin induces OSCC cell death via the *ERK/MAPK* pathway by curtailing cell viability, inhibiting cyclin *CDC2*, and disrupting cell migration.[30] The *JNK* pathway is equally pivotal in OSCC, and *JNK* phosphorylation levels are closely linked to higher differentiation phenotypes.[31] *JNK1*, a subtype of the *JNK* family, is particularly noteworthy.[32] Coronarin D affects the *JNK1/2* signaling pathway, promoting apoptosis and cell cycle arrest in 5-fluorouracil-resistant OSCC cell lines.[33] Hispolon exerts anti-OSCC effects by activating the *JNK* pathway through HO-1 upregulation, thereby inducing caspase-dependent apoptosis.[34] GO-Y078 activates the *p38/JNK1/2* pathway, enhancing *AP-1* DNA binding activity, leading to upregulating *HO-1* gene transcription and inhibiting OSCC cell growth.[35] In summary, the *ERK* and *JNK* branches of the *MAPK* pathway are crucial in OSCC.

Matrix metalloproteinases (MMPs) are crucial for degrading extracellular matrix proteins, a fundamental step in tumor migration and invasion, and are closely linked to angiogenesis.[36] Our study identified *MMP2* and *MMP9* as core target proteins for chlorogenic acid treatment of OSCC. In patients with OSCC, *MMP2* and *MMP9* activities were positively correlated with dipeptidyl peptidase IV mRNA levels, potentially regulating tumor metastasis.[37] In vitro studies have demonstrated that MicroRNA-29a upregulates *MMP2*, enhancing cancer invasion and anti-apoptosis capabilities.[38] Similarly, miR-31-5p elevates the *ERK-MMP9* cascade and targets *ACOX1*, positively affecting the cell motility linked to OSCC metastasis.[39] Treating OSCC cell lines with the *MMP2* inhibitor ARP101 markedly reduced cell proliferation and mobility.[40] Cordycepin significantly lowered *MMP2* and *MMP9* activities and *FAK* and *Akt* phosphorylation in a concentration-dependent manner, curbing migration and invasion of HSC-4 cells and inducing autophagy.[41] In mouse orthotopic tongue cancer models, halofuginone targeted cancer associated fibroblast inhibition, reduced *MMP2* expression and collagen deposition, and impeded OSCC migration and invasion.[42] *PAIP1* knockdown reduced *MMP9* activity and *SRC* phosphorylation, hindering OSCC cell formation and invasion.[43]

These findings suggest chlorogenic acid significantly influences the *MAPK-ERK* and *MAPK-JNK* signaling pathways during OSCC treatment. Apart from *ATM* and *BRAF*, the downregulation of core targets appears to be beneficial for OSCC patient survival. However, it is essential to note that network pharmacology primarily guides future research, and further experiments are required to validate these results.

5. Conclusion

In conclusion, chlorogenic acid's therapeutic strategy for OSCC might influence the *MAPK-ERK* and *MAPK-JNK* pathways by targeting *ESR1, MMP2, MMP9, SRC, MAPK8, MAPK1, CDC42, ERBB2, ATM,* and *BRAF*. This intervention could inhibit cell migration, invasion, growth, and apoptosis. This study introduces a novel perspective and strategy for researching targeted therapy mechanisms.

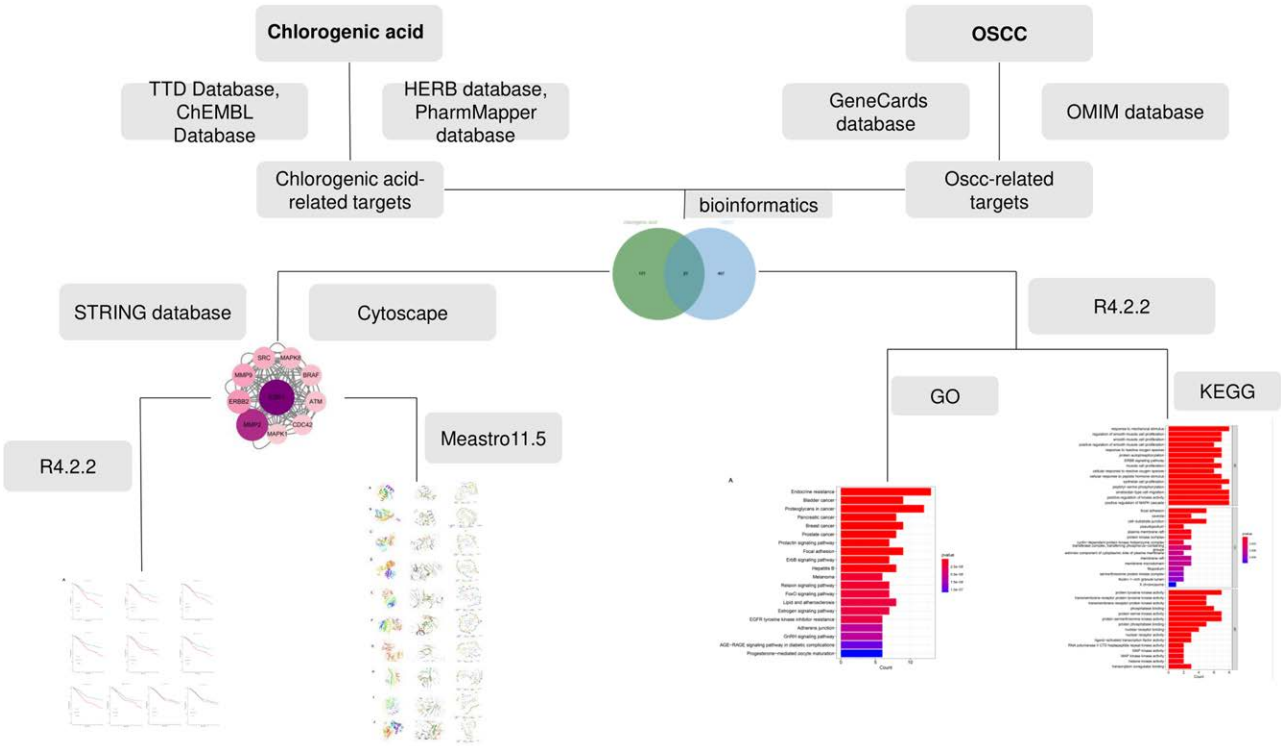

Figure 6. Flow chart of experimental research on drug treatment of disease. GO = Gene Ontology, KEGG = Kyoto Encyclopedia of Genes and Genomes, OMIM = Online Mendelian Inheritance in Man CC cell component ESR1 estrogen receptor, OSCC = oral squamous cell carcinoma.

Acknowledgments

We would like to thank all the participants for their outstanding contributions, as well as the Therapeutic Target Database, ChEMBL Database, HERB Database, PharmMapper Database, SwissTarget prediction screening medium, OMIM database, and GeneCards, which supported our experimental research.

Author contributions

Conceptualization: Yutao Yang.
Data curation: Xulong Xve.
Formal analysis: Zhanqin Feng.
Funding acquisition: Zhanqin Feng.
Investigation: Zhanqin Feng.
Methodology: Zhanqin Feng, Puyu Hao.
Project administration: Jun Zhang.
Resources: Jun Zhang.
Software: Yutao Yang.
Validation: Yutao Yang.
Visualization: Xulong Xve.
Writing – original draft: Zhanqin Feng, Puyu Hao.
Writing – review & editing: Jun Zhang.

References

[1] Chai AWY, Lim KP, Cheong SC. Translational genomics and recent advances in oral squamous cell carcinoma. Semin Cancer Biol. 2020;61:71–83.
[2] Bugshan A, Farooq I. Oral squamous cell carcinoma: metastasis, potentially associated malignant disorders, etiology and recent advancements in diagnosis. F1000Res. 2020;9:229.
[3] Huang TH, Li KY, Choi WS. Lymph node ratio as prognostic variable in oral squamous cell carcinomas: systematic review and meta-analysis. Oral Oncol. 2019;89:133–43.
[4] Gharat SA, Momin M, Bhavsar C. Oral squamous cell carcinoma: current treatment strategies and nanotechnology-based approaches for prevention and therapy. Crit Rev Ther Drug Carrier Syst. 2016;33:363–400.
[5] Li X, Guo S, Xiong X-K, et al. Combination of quercetin and cisplatin enhances apoptosis in OSCC cells by downregulating xIAP through the NF-κB pathway. J Cancer. 2019;10:4509–21.
[6] Menditti D, Santagata M, Imola G, et al. Personalized medicine in oral oncology: imaging methods and biological markers to support diagnosis of Oral Squamous Cell Carcinoma (OSCC): a narrative literature review. J Pers Med. 2023;13:1397.
[7] Pimpley V, Patil S, Srinivasan K, Desai N, Murthy PS. The chemistry of chlorogenic acid from green coffee and its role in attenuation of obesity and diabetes. Prep Biochem Biotechnol. 2020;50:969–78.
[8] Naveed M, Hejazi V, Abbas M, et al. Chlorogenic acid (CGA): a pharmacological review and call for further research. Biomed Pharmacother. 2018;97:67–74.
[9] Santana-Gálvez J, Cisneros-Zevallos L, Jacobo-Velázquez DA. Chlorogenic acid: recent advances on its dual role as a food additive and a nutraceutical against metabolic syndrome. Molecules. 2017;22:358.
[10] Lu H, Tian Z, Cui Y, Liu Z, Ma X. Chlorogenic acid: a comprehensive review of the dietary sources, processing effects, bioavailability, beneficial properties, mechanisms of action, and future directions. Compr Rev Food Sci Food Saf. 2020;19:3130–58.
[11] Sharma G, Kamboj M, Narwal A, Bhardwaj R, Yadav P. Cytotoxic role of chlorogenic acid on oral squamous cell carcinoma cell line. Indian J Otolaryngol Head Neck Surg. 2022;74:5773–81.
[12] Gupta A, Atanasov AG, Li Y, Kumar N, Bishayee A. Chlorogenic acid for cancer prevention and therapy: current status on efficacy and mechanisms of action. Pharmacol Res. 2022;186:106505.
[13] Jiang Y, Kusama K, Satoh K, Takayama E, Watanabe S, Sakagami H. Induction of cytotoxicity by chlorogenic acid in human oral tumor cell lines. Phytomedicine. 2000;7:483–91.
[14] Nabavi SF, Tejada S, Setzer WN, et al. Chlorogenic acid and mental diseases: from chemistry to medicine. Curr Neuropharmacol. 2017;15:471–9.
[15] Zhao L, Zhang H, Li N, et al. Network pharmacology, a promising approach to reveal the pharmacology mechanism of Chinese medicine formula. J Ethnopharmacol. 2023;309:116306.
[16] Sun S, Wang J, Liu J, et al. MiR-302b suppresses tumor metastasis by targeting frizzled 6 in OSCC. J Dent Res. 2021;100:739–45.
[17] Wang Q, Zhi Y, Ren W, et al. Suppression of OSCC malignancy by oral glands derived-PIP identified by iTRAQ combined with 2D LC-MS/MS. J Cell Physiol. 2019;234:15330–41.

[18] Miao M, Xiang L. Pharmacological action and potential targets of chlorogenic acid. Adv Pharmacol. 2020;87:71–88.
[19] Wagner EF, Nebreda AR. Signal integration by JNK and p38 MAPK pathways in cancer development. Nat Rev Cancer. 2009;9:537–49.
[20] Ullah R, Yin Q, Snell AH, Wan L. RAF-MEK-ERK pathway in cancer evolution and treatment. Semin Cancer Biol. 2022;85:123–54.
[21] Weston CR, Davis RJ. The JNK signal transduction pathway. Curr Opin Cell Biol. 2007;19:142–9.
[22] Park J-I. MAPK-ERK pathway. Int J Mol Sci. 2023;24:9666.
[23] Zhao T-C, Zhou Z-H, Ju W-T, et al. Mechanism of sensitivity to cisplatin, docetaxel, and 5-fluorouracil chemoagents and potential erbB2 alternatives in oral cancer with growth differentiation factor 15 overexpression. Cancer Sci. 2022;113:478–88.
[24] Alkhatib DZR, Thi Kim Truong T, Fujii S, et al. Stepwise activation of p63 and the MEK/ERK pathway induces the expression of ARL4C to promote oral squamous cell carcinoma cell proliferation. Pathol Res Pract. 2023;246:154493.
[25] Hsieh M-J, Ho H-Y, Lo Y-S, et al. Semilicoisoflavone B induces apoptosis of oral cancer cells by inducing ROS production and downregulating MAPK and Ras/Raf/MEK signaling. Int J Mol Sci. 2023;24:4505.
[26] Yun H-M, Kwon Y-J, Kim E, Chung H-J, Park K-R. Machilin D promotes apoptosis and autophagy, and inhibits necroptosis in human oral squamous cell carcinoma cells. Int J Mol Sci. 2023;24:4576.
[27] Kumar VB, Hsieh M-J, Mahalakshmi B, et al. 7-Epitaxol induces apoptosis and autophagy in head and neck squamous cell carcinoma through inhibition of the ERK pathway. Cells. 2021;10:2633.
[28] Yao C, Kong F, Zhang S, Wang G, She P, Zhang Q. Long noncoding RNA BANCR promotes proliferation and migration in oral squamous cell carcinoma via MAPK signaling pathway. J Oral Pathol Med. 2021;50:308–15.
[29] Greer PFC, Rich A, Coates DE. Effects of galectin-1 inhibitor OTX008 on oral squamous cell carcinoma cells in vitro and the role of AP-1 and the MAPK/ERK pathway. Arch Oral Biol. 2022;134:105335.
[30] Chen Q, Song S, Wang Z, et al. Isorhamnetin induces the paraptotic cell death through ROS and the ERK/MAPK pathway in OSCC cells. Oral Dis. 2021;27:240–50.
[31] Gkouveris I, Nikitakis N, Avgoustidis D, Karanikou M, Rassidakis G, Sklavounou A. ERK1/2, JNK and STAT3 activation and correlation with tumor differentiation in oral SCC. Histol Histopathol. 2017;32:1065–76.
[32] Wu Q, Wu W, Fu B, Shi L, Wang X, Kuca K. JNK signaling in cancer cell survival. Med Res Rev. 2019;39:2082–104.
[33] Hsieh M-Y, Hsieh M-J, Lo Y-S, et al. Modulating effect of Coronarin D in 5-fluorouracil resistance human oral cancer cell lines induced apoptosis and cell cycle arrest through JNK1/2 signaling pathway. Biomed Pharmacother. 2020;128:110318.
[34] Yang W-E, Chen Y-T, Su C-W, et al. Hispolon induces apoptosis in oral squamous cell carcinoma cells through JNK/HO-1 pathway activation. J Cell Mol Med. 2023;27:1250–60.
[35] Chien M-H, Shih P-C, Ding Y-F, et al. Curcumin analog, GO-Y078, induces HO-1 transactivation-mediated apoptotic cell death of oral cancer cells by triggering MAPK pathways and AP-1 DNA-binding activity. Expert Opin Ther Targets. 2022;26:375–88.
[36] Pittayapruek P, Meephansan J, Prapapan O, Komine M, Ohtsuki M. Role of matrix metalloproteinases in photoaging and photocarcinogenesis. Int J Mol Sci. 2016;17:868.
[37] Talebi Taheri A, Lashkarbolouki T, Karimi A, Sirati-Sabet M, Karima S, Goudarzi A. Comparison of DPPIV levels in serum and tumour of OSCC patients and its correlation with active matrix metalloproteinases 2 and 9. Asian Pac J Cancer Prev. 2023;24:1343–9.
[38] Lu L, Xue X, Lan J, et al. MicroRNA-29a upregulates MMP2 in oral squamous cell carcinoma to promote cancer invasion and anti-apoptosis. Biomed Pharmacother. 2014;68:13–9.
[39] Lai Y-H, Liu H, Chiang W-F, et al. MiR-31-5p-ACOX1 axis enhances tumorigenic fitness in oral squamous cell carcinoma via the promigratory prostaglandin E2. Theranostics. 2018;8:486–504.
[40] Celentano A, Yap T, Paolini R, et al. Inhibition of matrix metalloproteinase-2 modulates malignant behaviour of oral squamous cell carcinoma cells. J Oral Pathol Med. 2021;50:323–32.
[41] Binlateh T, Uppatcha N, Thepchai J, et al. Cordycepin attenuates migration and invasion of HSC-4 oral squamous carcinoma cells through autophagy-dependent FAK/Akt and MMP2/MMP9 suppression. J Dent Sci. 2022;17:1677–88.
[42] Wang D, Tian M, Fu Y, et al. Halofuginone inhibits tumor migration and invasion by affecting cancer-associated fibroblasts in oral squamous cell carcinoma. Front Pharmacol. 2022;13:1056337.
[43] Swarup N, Hong K-O, Chawla K, et al. Effect of PAIP1 on the metastatic potential and prognostic significance in oral squamous cell carcinoma. Int J Oral Sci. 2022;14:9.